

SUPPORTING INFORMATION

Engineering co-drug solid forms: the mechanochemical synthesis of an indomethacin-caffeine system

Simone Bordignon,¹ Paolo Cerreia Vioglio,¹ Emanuele Priola,¹ Dario Voinovich,² Roberto Gobetto^{1}, Yusuke Nishiyama³ and Michele R. Chierotti^{1*}*

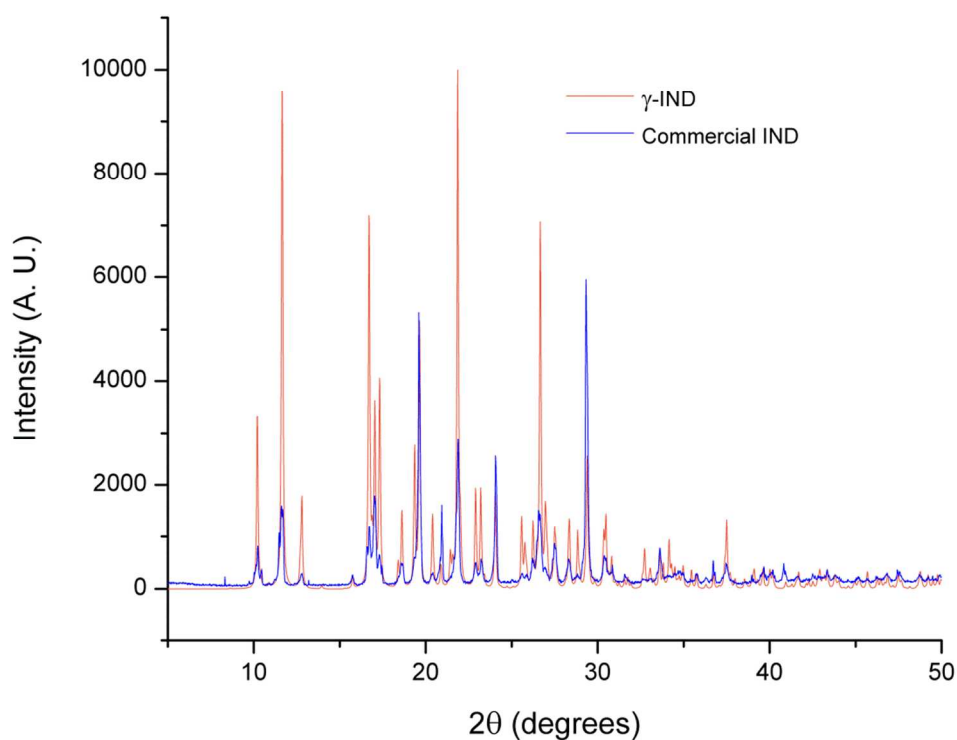


Figure S1. Comparison between γ -IND (red) and commercial IND (blue) PXR D patterns.

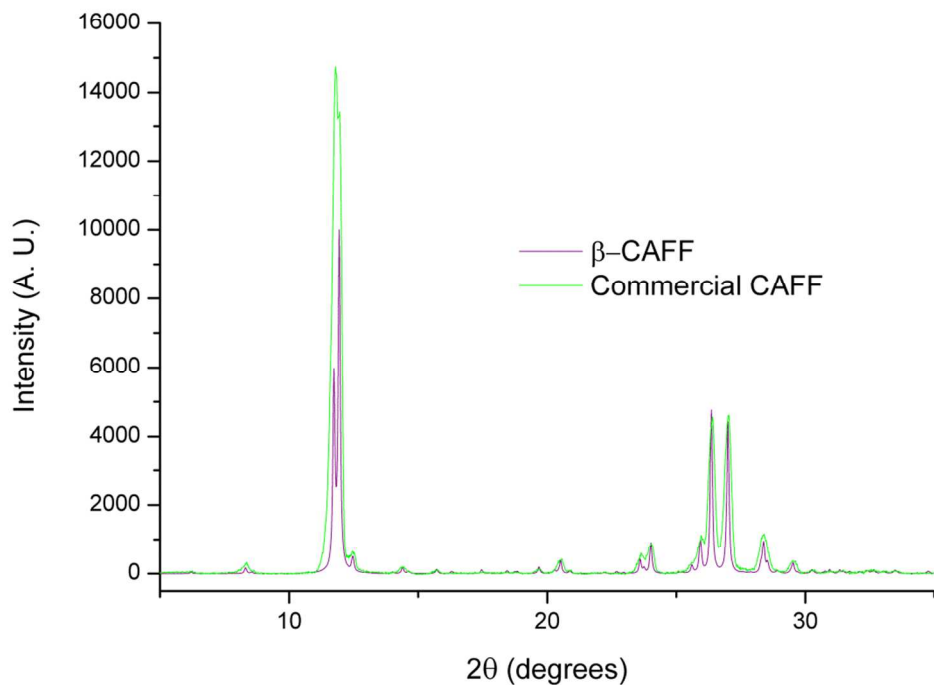


Figure S2. Comparison between β -CAFF (violet) and commercial CAFF (green) PXRD patterns.

Table S1. Values of distances and angles between atoms in IND·CAFF X-ray structure. Refer to Figure S3 for atom numeration.

Distance (Å)		Angle (°)	
C11-C1	1.735(2)	C2-C3-C4	121.23(18)
C3-C2	1.384(3)	C3-C4-C5	118.59(18)
C4-C7	1.488(3)	C3-C4-C7	122.55(16)
O6-C18	1.315(2)	O2-C23-N4	121.70(19)
O4-C7	1.215(2)	O2-C23-N3	121.63(19)
O5-C18	1.198(2)	C22-N3-C24	120.48(17)
O2-C23	1.214(2)	C21-N1-C22	103.25(17)
O1-C27	1.227(2)	C14-C15-N5	130.57(17)
O3-C12	1.372(2)	C11-C10-C9	132.11(17)
O3-C19	1.422(3)	N2-C20-C27	131.01(18)

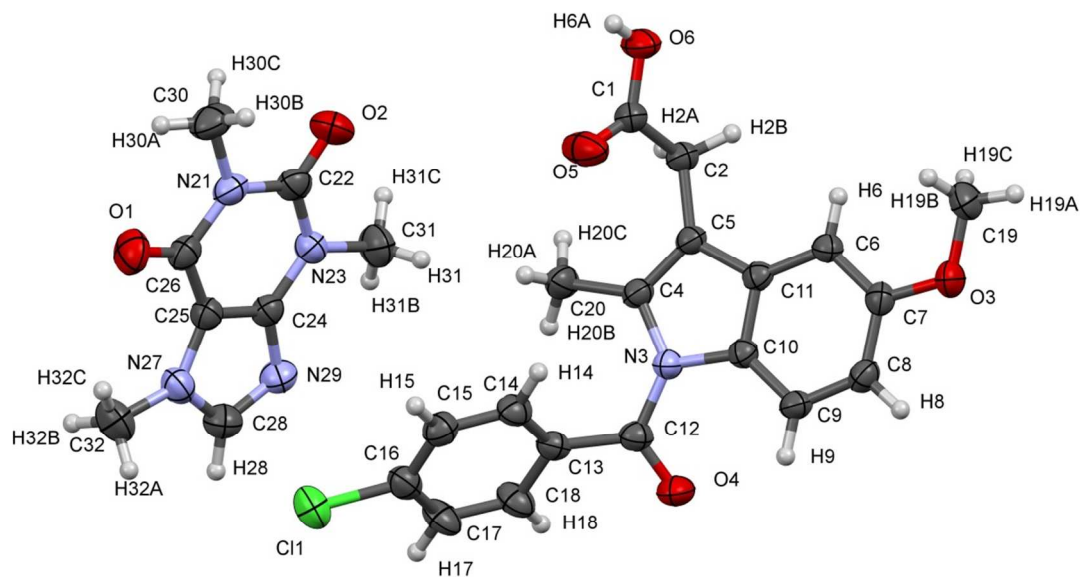


Figure S3. Asymmetric unit of IND·CAFF, with atom numeration. Thermal ellipsoids drawn at 70% of probability. (C = grey; H = white; O = red; N = azure; Cl = green).

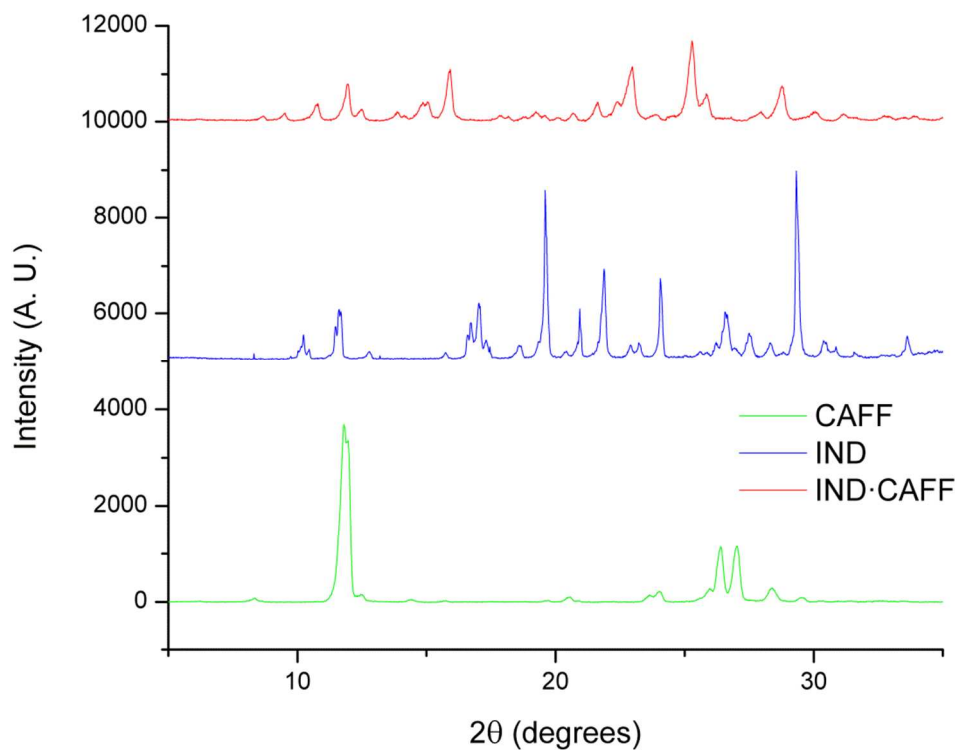


Figure S4. Comparison of PXRD patterns: IND·CAFF (red), IND (blue) and CAFF (green).

Vibrational spectroscopies

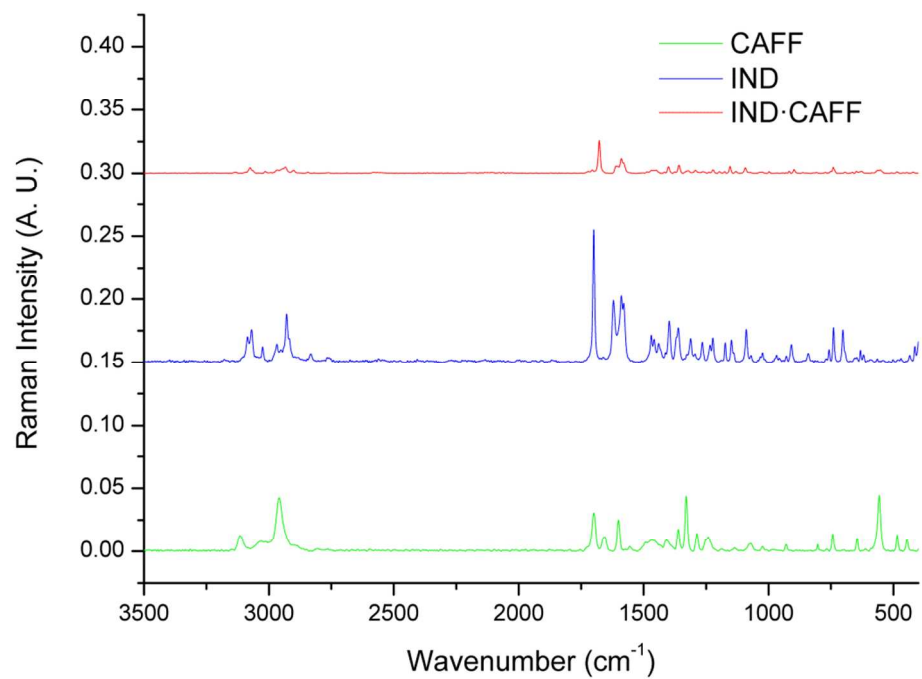


Figure S5. Comparison between Raman spectra of IND·CAFF (red), CAFF (green) and IND (blue).

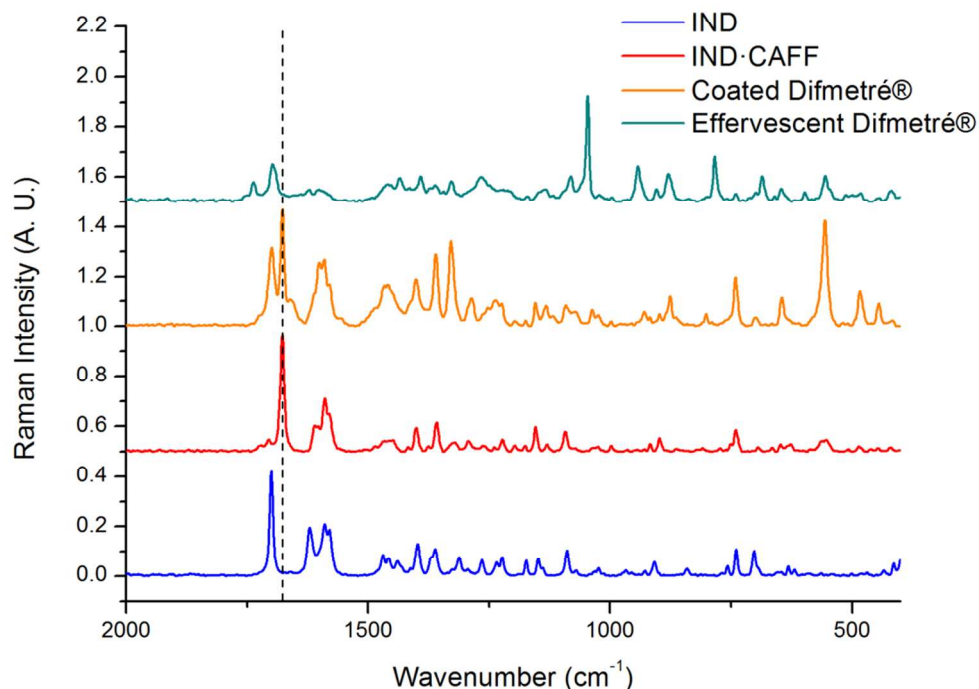


Figure S6. Comparison between Raman spectra of IND (blue), IND·CAFF (red), film-coated Difmetré® tablet (orange) and effervescent Difmetré® tablet (turquoise). The dotted line highlights an IND·CAFF characteristic band.

IR-ATR characterization

Figure S7 (whole spectra) and Figure 3 (1800-1100 cm⁻¹ region, see main text) show a comparison between the IR-ATR spectra of the co-drug and the starting materials. It is possible to observe changes in the O-H stretching region (at about 3000 cm⁻¹) of IND·CAFF because of the formation of a HB (O-H···N) that is different from the one in pure γ -IND (O-H···O). Furthermore, the stretching band associated to the carboxylic C=O of the acid moiety of IND moves from 1711 cm⁻¹ in the pure API¹ to higher wavenumbers (1718 cm⁻¹), as well as the C=N band of CAFF, which shifts from 1598 cm⁻¹ in the starting material² to 1601 cm⁻¹ in the co-drug, following the formation of the new HB.

Notably, in the spectrum of the co-drug there is no evidence of a protonic transfer. In fact, the signal at 1483 cm⁻¹, which is typically medium-weak for a NH⁺ deformation mode in a salt, appears as a strong peak in the spectrum of IND·CAFF and it is most likely due to a CCH deformation mode; the same can be said about the signal at about 1235 cm⁻¹, ascribable to an *in-plane* CH deformation. At 737 cm⁻¹ we observe the typical signal of a COOH *out-of-plane* deformation, while there is no trace of the characteristic peak at 1370 cm⁻¹, attributed to the asymmetric stretching of COO⁻ in salts.³ These considerations imply the neutral nature of the adduct.

Finally, it is possible to observe significant differences in the fingerprint region (under 1000 cm⁻¹). All these changes suggested that IND·CAFF consisted in a new crystalline form, different from the ones it was produced from.

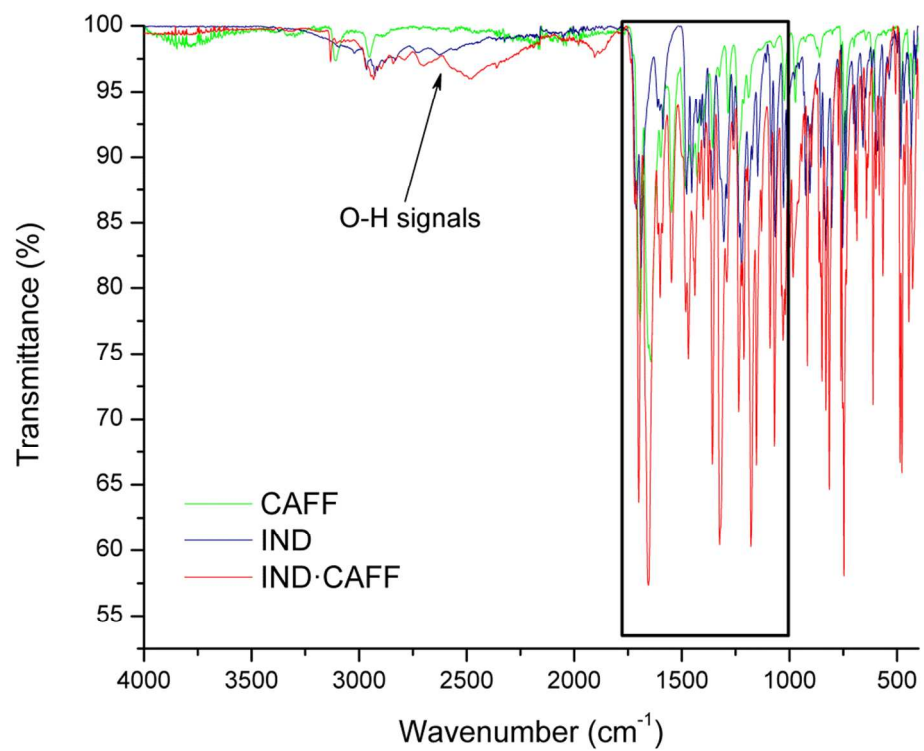


Figure S7. Comparison between IR-ATR spectra of IND·CAFF (red), CAFF (green) and IND (blue). The highlighted region is shown in Figure 3 (see main text).

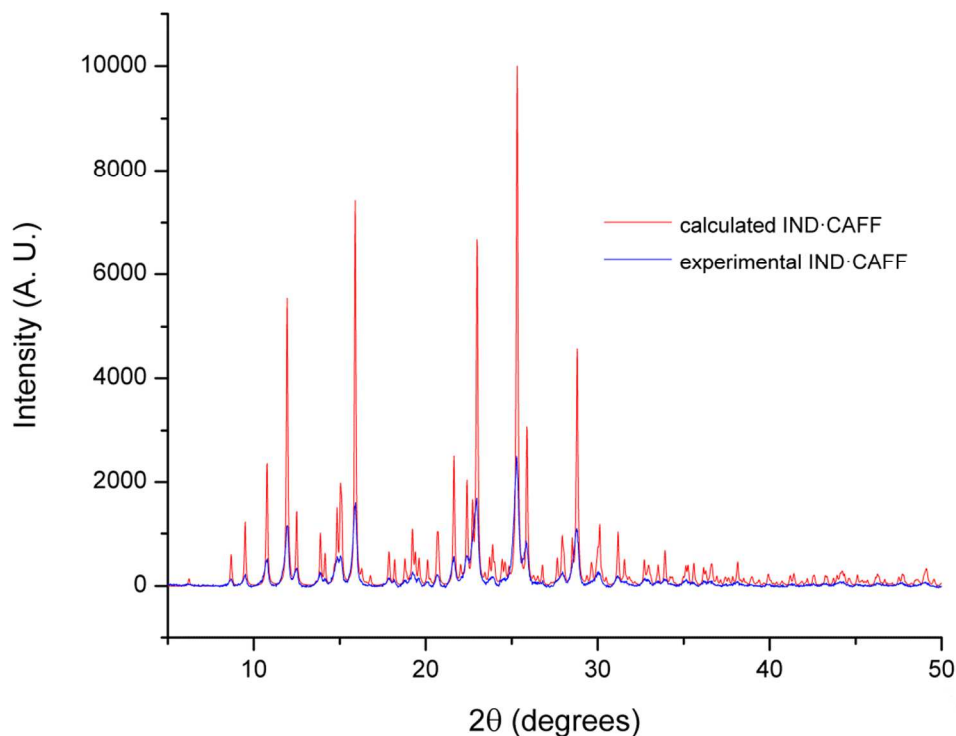


Figure S8. Comparison between calculated (red) and experimental (blue) IND-CAFF PXRD patterns.

SSNMR characterization

The ^{13}C CPMAS spectrum of IND-CAFF (Figure 5) shows a high degree of crystallinity (FWHM around 85–90 Hz) and the number of peaks confirms the presence of one independent molecule for each co-former in the unit cell, in nice agreement with SCXRD data. Both CAFF and IND resonances undergo major shifts, thus confirming the occurrence of a novel crystalline form. More importantly, the signal at 179.0 ppm in pure γ -IND, characteristic of the $\text{COOH}\cdots\text{HOOC}$ dimeric homosynthon, is affected by a 7.2 ppm shift to low frequencies. This is due to the formation of a new $\text{COOH}\cdots\text{N29}$ HB interaction, in which the hydrogen atom is located on the carboxylic group rather than the nitrogen atom. This confirms the product to be a cocrystal and not a salt, in accordance with the XRD structure. In the ^{15}N CPMAS spectrum (Figure 6) it is possible to observe a number of signals corresponding to the sum of the nitrogen atoms of the molecules of the reagents, confirming the presence of a single independent molecule of each in the unit cell. The most significant shift is the one that leads the partially split signal, related to the purinic nitrogen atom of CAFF, from 230.0 ppm in the pure reagent to 213.0 ppm in the adduct. This is symptomatic of the formation of a HB involving the nitrogen atom. In general, shifts toward low frequencies are expected with an entity of 10–20 ppm for HB formation and up to 90–100 ppm for salification. They are due to the minor contribution of the lone electronic pair to the $\sigma_{\text{para}}^{\text{para}}_{\text{loc}}$ term of chemical shift, being it removed by quaternarization.

The ^{13}C CPMAS spectrum of Difmetré® (film-coated tablet) is characterized by signals of pure γ -IND, pure CAFF and IND-CAFF beside those of the excipients which are predominant. Accordingly to

the very little amount present in Difmetré® (about 0.6% w/w), prochlorperazine dimaleate is not visible.

2D SSNMR experiments

Table S2. Detailed ^{13}C and ^{15}N SSNMR experimental acquisition parameters.

nuclei	IND			CAFF			IND-CAFF		
	^1H	^{13}C	^{15}N	^1H	^{13}C	^{15}N	^1H	^{13}C	^{15}N
window/kHz	100	36.8	26.3	100	36.8	26.3	70.4	36.8	26.3
points ^a	4096	1834	1576	2048	2568	1576	2048	2936	2102
scans	3	256	4096	3	1024	256	3	256	1024
recycle delay/s	7	15	15	47	60	80	20	10	10

^aComplex time-domain data points.

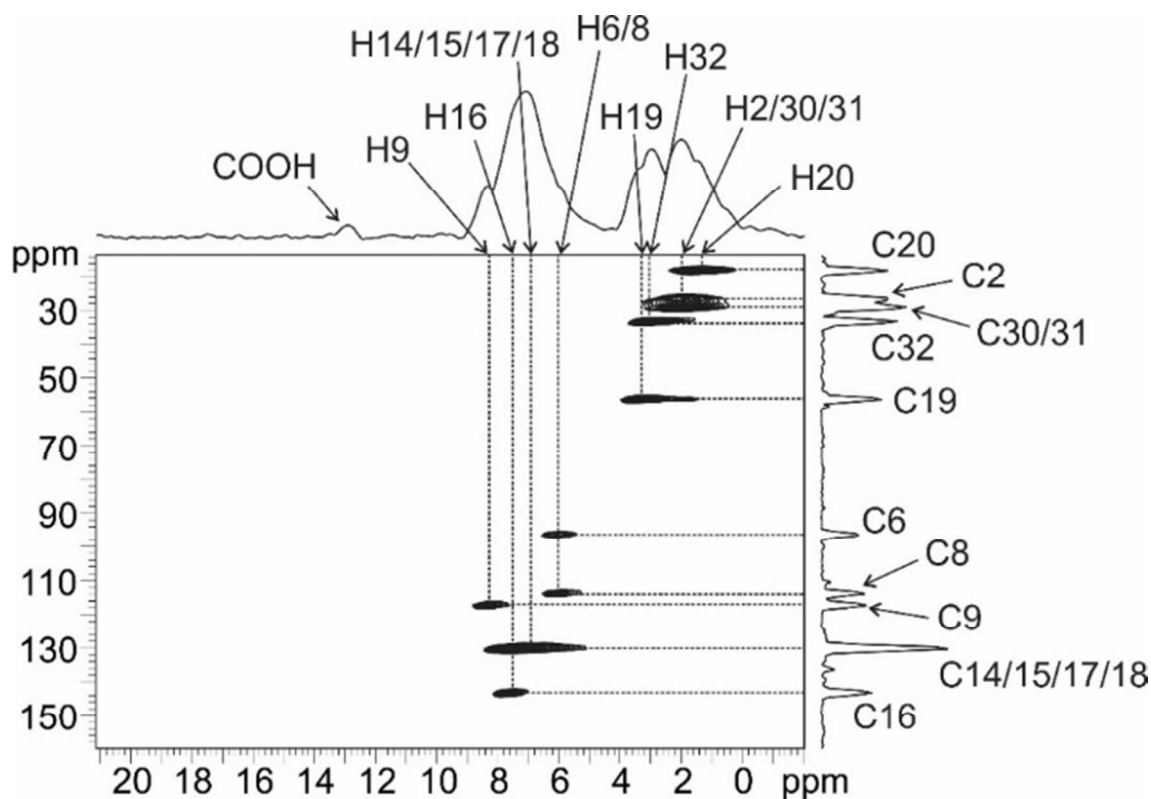


Figure S9. ^1H - ^{13}C HETCOR 2D spectrum of IND-CAFF. On the left, the protonic spectrum, in the range -2 to 21 ppm, is shown, while the upper one is a ^{13}C spectrum, in the range 25 to 160 ppm (spinning speed: 70 kHz, room temperature). Dotted lines stand for correlations between protons covalently bonded to carbon atoms.

In Figure S10, we can see protonic signal intensities at different excitation times in ^{14}N - ^1H D-HMQC (Figure S10a) and J-HMQC (Figure S10b). As for the D-version, re-introducing the dipolar interaction between ^1H and ^{14}N nuclei determines a great increase in sensitivity. This is due to the dipolar nature of the correlations observed. In J-HMQC, we do not observe signals at any of the investigated values of τ . Moreover, in order to demonstrate that the lack of signal is not due to short coherence life time (T_2'), a

comparison with Pigment Yellow 138 was made. It is characterized by the presence of an N-H covalent bond in its structure and gave a signal in the J-HMQC spectrum.⁴ Notably, it presents a T_2' value (2.1 ms) for the NH signal which is even shorter than that of the OH signal in IND·CAFF (3.1 ms). Thus, by considering very similar build up curves, in principle the presence of a J coupling in IND·CAFF should have generated a peak. Furthermore, the optimal excitation time is given by $1/(2J+2RDS)$. If we assume $^1J(^{14}\text{N}-^1\text{H}) \approx 70$ Hz and $D_{RDS}(^{14}\text{N}-^1\text{H}) \approx 110$ Hz, both reasonable and conservative values according to Cavadini et al.,⁵ the optimal excitation time is 2.8 ms. For IND·CAFF, it corresponds to more than 10% of residual magnetization. All this indirectly proves the carboxylic proton of IND and the N29 atom of CAFF not to be covalently bonded. Consequently, the residual dipolar splitting (RDS) is not sufficient alone for transferring magnetization to give correlation signals.

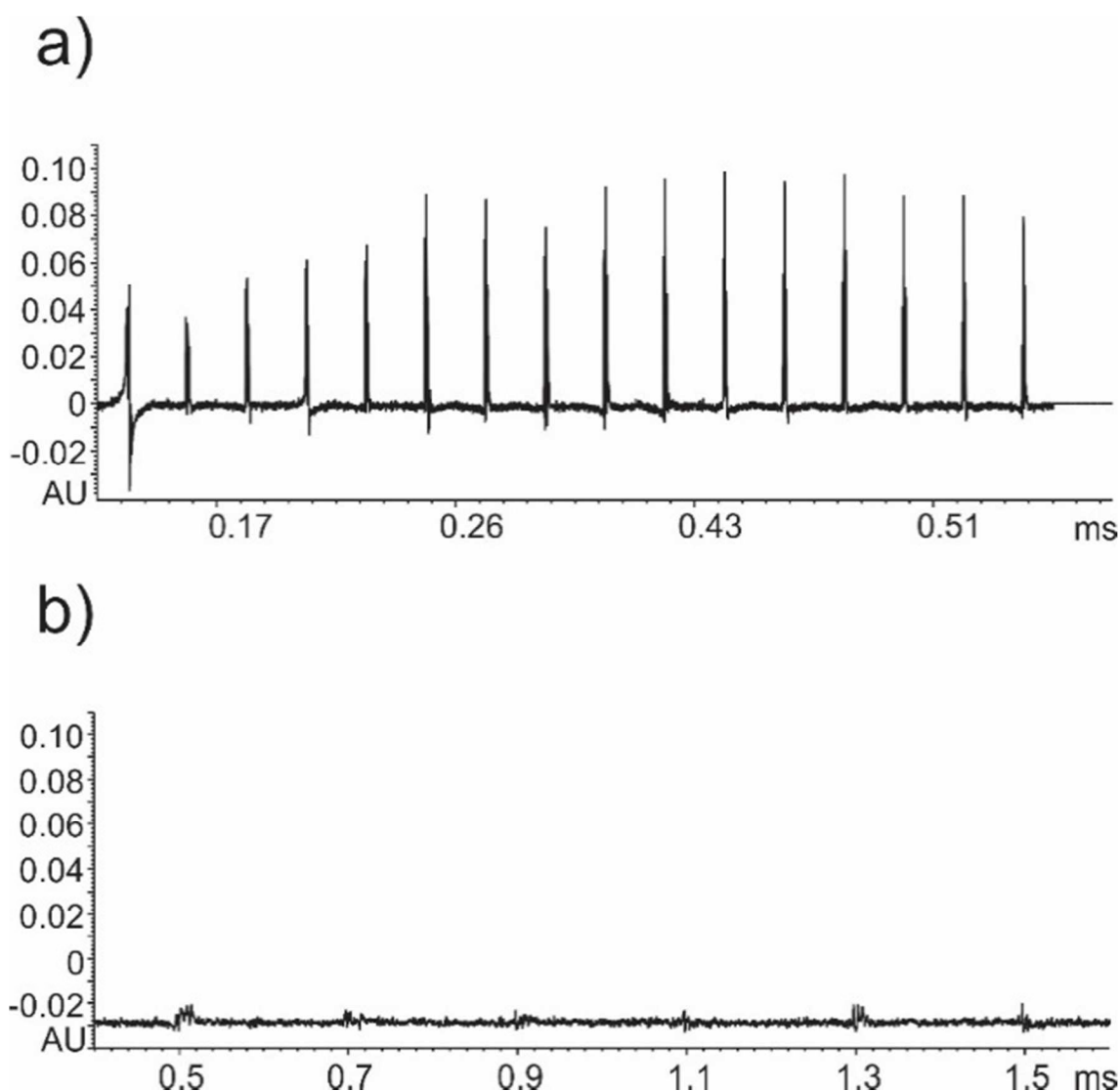


Figure S10. 1D $^{14}\text{N}-^1\text{H}$ HMQC spectra of IND·CAFF at different excitation times (τ_{exc}): a) D-version and b) J-version. In the first case, the dipolar recoupling determines the observation of signals which increase in the S/N ratio as a function of the recoupling time (τ_{exc}). In the second case, no signal is observed for any τ_{exc} when the magnetization transfer occurs through J-coupling or RDS.

The 2D ^{14}N - ^1H D-HMQC spectrum (Figure S11) displays intense correlations between the methyl protons of CAFF and the nitrogen atoms to which each methyl group is linked. We can also see how the N27 and N29 atoms of CAFF interact with aromatic ^1H nuclei. The most significant correlation, though, is the one between the carboxylic OH of IND and the N29 atom of CAFF. This perfectly agrees with the data obtained from SCXRD analysis. The low intensity of the signal is symptomatic of the dipolar nature of the interaction, as expected. Table S3 reports the observed correlations. See Figure S3 as a reference for the numeration of nitrogen atoms.

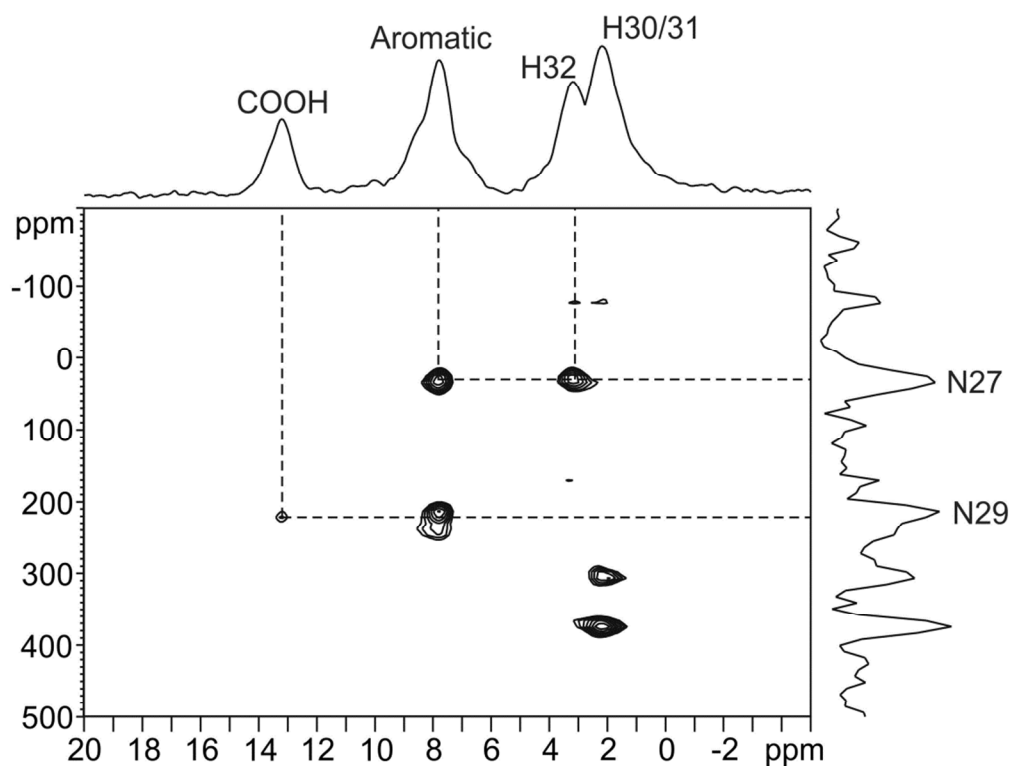


Figure S11. ^{14}N - ^1H D-HMQC 2D spectrum of IND-CAFF. The upper spectrum is the ^1H mono-dimensional experiment (range: -5 to 20 ppm) while on the right the ^{14}N spectrum, in the range -200 to 500 ppm, is depicted (spinning speed: 70 kHz, room temperature). Dotted lines stand for correlations between protons and nitrogen atoms in the crystalline structure. The experiment was repeated with the same experimental parameters in order to individuate fake correlations generated by t_1 noise (unassigned peaks).

Table S3. Significant correlations between proximal protons and ^{14}N nuclei in the structure of the co-drug, as pointed out by the ^{14}N - ^1H D-HMQC experiment (Figure S11).

^{14}N - ^1H D-HMQC
Spatial correlations
H32-N27
N27-Aromatic ^1H
N29-Aromatic ^1H
COOH-N29

In order to get spectroscopic insights on cocrystal formation, packing and HB interactions at play in the crystalline structure of IND·CAFF,⁶ a ¹H DQ MAS experiment was run. The presence of DQ transitions between couple of protonic spins implies their spatial proximity, within 3 Å, in the structure.⁷ The spectrum is reported in Figure S12, while the ensuing results are shown in Table S4. As we can see from the spectrum, the H28 and H32 protons of CAFF correlate, giving rise to a DQ signal. More significantly, the carboxylic proton of IND, directly involved in the characteristic HB of the co-drug, finds itself close to H28 and H31 of CAFF. This is confirmed by the presence of correlation peaks in the 2D spectrum and is in accordance with the crystal structure data.

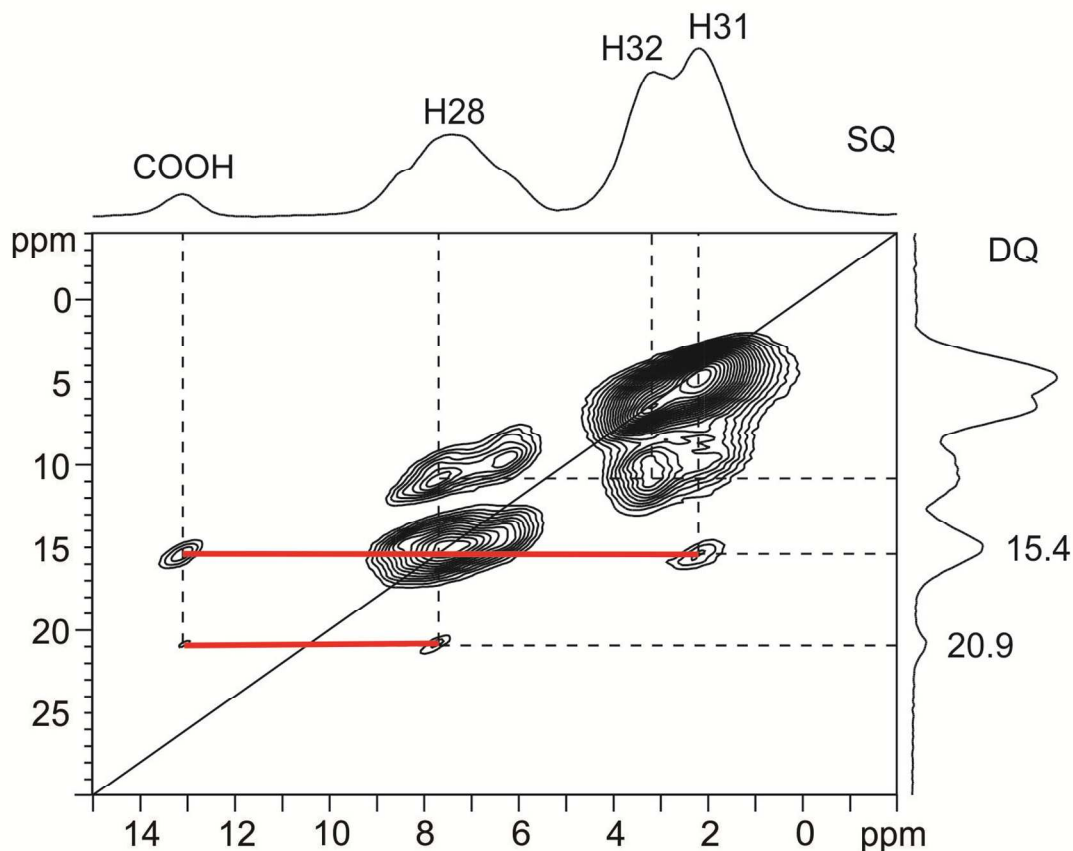


Figure S12. ¹H DQ BABA spectrum (spinning speed = 70 kHz) of IND·CAFF. The ¹H MAS spectrum is plotted along the F2 (horizontal) axis and a double quantum skyline projection is shown along the F1 (vertical) axis. Key correlations are noted on the spectrum. Spectra were obtained at 14.1 T and 273 K.

Table S4. Significant correlations between close protons in the structure of the co-drug, as pointed out by the ¹H DQ MAS experiment (Figure S12).

¹ H DQ MAS	SQ	SQ	DQ
Spatial correlations			
COOH-H31	13.1	2.3	15.4
COOH-H28	13.1	7.8	20.9
H28-H32	7.8	3.2	11.0

Thermal analysis

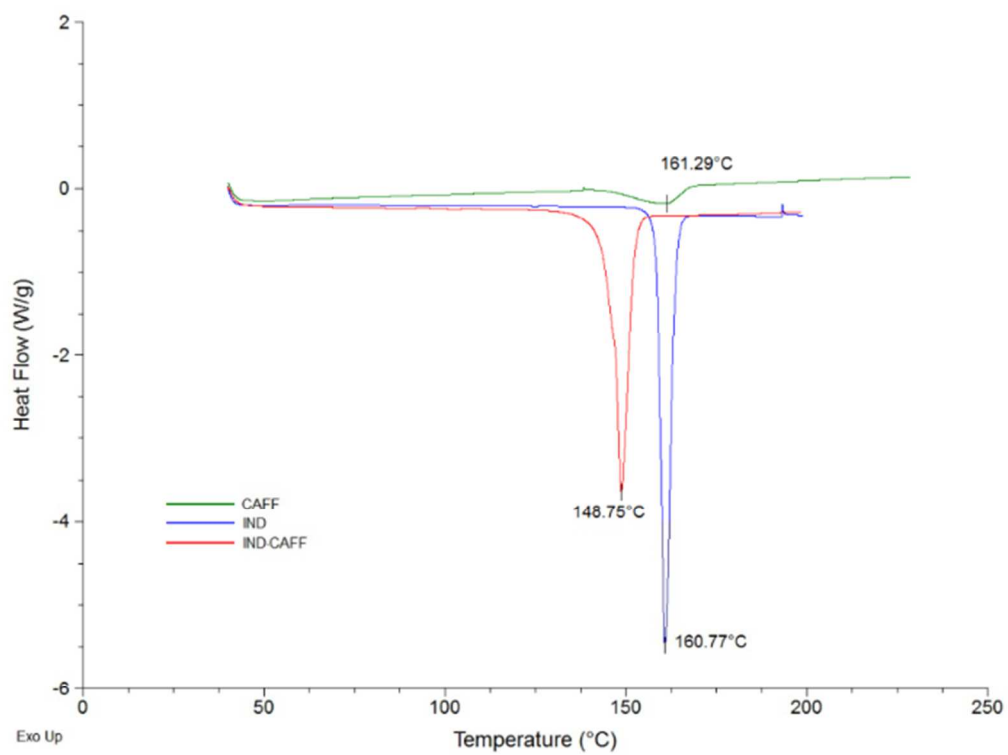


Figure S13. Comparison between the DSC curves of CAFF (green), IND (blue) and IND·CAFF (red).

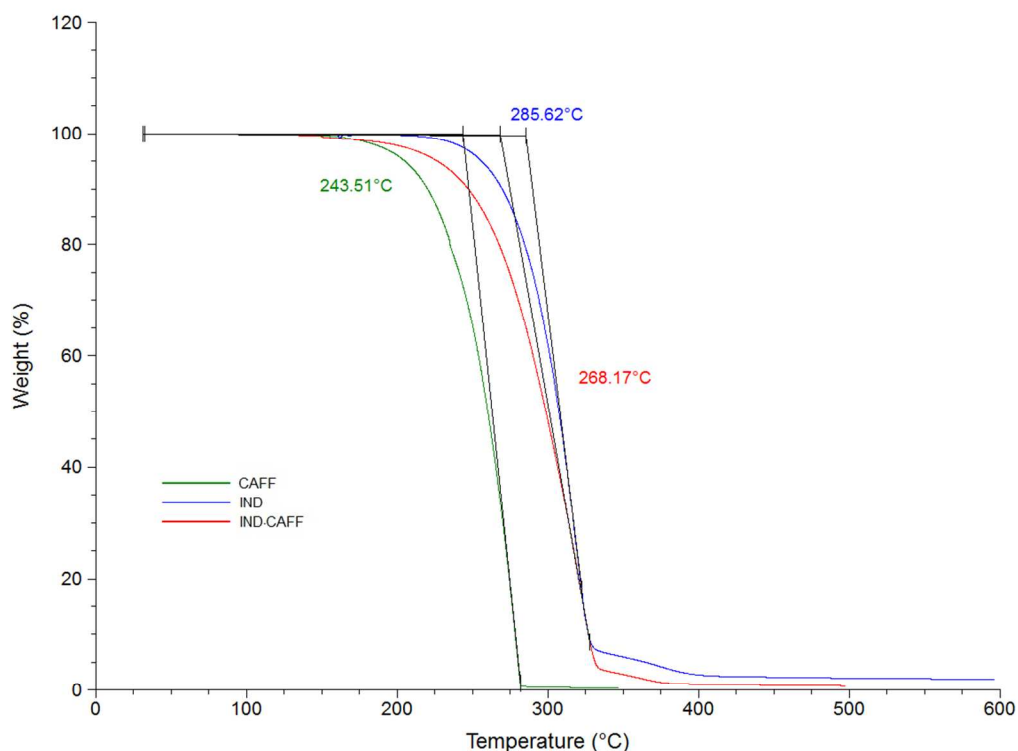


Figure S14. Comparison between the thermogravimetric curves of CAFF (green), IND (blue) and IND·CAFF (red).

References

- (1) Ali, H. R. H.; Alhalaweh, A.; Velaga, S. P. *Drug Dev. Ind. Pharm.* **2013**, *39*, 625–634.
- (2) Srivastava, S. K.; Singh, V. B. *Spectrochim. Acta. A. Mol. Biomol. Spectrosc.* **2013**, *115*, 45–50.
- (3) Ali, H. R. H.; Alhalaweh, A.; Mendes N. F. C.; Ribeiro-Claro P.; Velaga S. P. *CrystEngComm* **2012**, *14*, 6665–6674.
- (4) Gumbert, S. D.; Korbitzer, M.; Alig, E.; Schmidt, M. U.; Chierotti, M. R.; Gobetto, R.; Li, X. Z.; van de Streek, J. *Dyes Pigm.* **2016**, *131*, 364–372.
- (5) Cavadini, S.; Antonijevic, S.; Lupulescu, A.; Bodenhausen, G.; *J. Magn. Reson.* **2006**, *182*, 168–172.
- (6) Goward, G. R.; Schnell, I.; Brown, S. P.; Spiess, H. W.; Kim, H.; Ishida, H. *Magn. Reson. Chem.* **2001**, *39*, S5–S17.
- (7) Brown, S. P.; Spiess, H. W. *Chem. Rev.* **2001**, *101*, 4125–4156.